THE JOURNAL OF BIOLOGICAL CHEMISTRY VOL. 290, NO. 18, pp. 11393–11402, May 1, 2015
© 2015 by The American Society for Biochemistry and Molecular Biology, Inc. Published in the U.S.A.

Pathogenic Mutations Differentially Affect the Catalytic Activities of the Human B_{12}-processing Chaperone CblC and Increase Futile Redox Cycling*

Received for publication, January 7, 2015, and in revised form, March 16, 2015 Published, JBC Papers in Press, March 25, 2015, DOI 10.1074/jbc.M115.637132

Carmen Gherasim, Markus Ruetz, Zhu Li, Stephanie Hudolin, and Ruma Banerjee[1]

From the Department of Biological Chemistry, University of Michigan Medical Center, Ann Arbor, Michigan 48109-0600

Background: CblC processes cobalamins entering a cell to a common intermediate.
Results: Pathogenic mutations at Arg-161 weaken glutathione binding to CblC and stabilize cob(II)alamin.
Conclusion: The R161Q/G mutations impair the dealkylation but not the decyanation activity of CblC.
Significance: Increased redox cycling by the CblC mutants explains the observed cellular oxidative stress associated with this disorder.

Human CblC catalyzes the elimination of the upper axial ligand in cobalamin or B_{12} derivatives entering the cell from circulation. This processing step is critical for assimilation of dietary cobalamin into the active cofactor forms that support the B_{12}-dependent enzymes, methionine synthase and methylmalonyl-CoA mutase. Using a modified nitroreductase scaffold tailored to bind cobalamin and glutathione, CblC exhibits versatility in the mechanism by which it removes cyano *versus* alkyl ligands in cobalamin. In this study, we have characterized the effects of two pathogenic missense mutations at the same residue, R161G and R161Q, which are associated with early and late onset of the CblC disorder, respectively. We find that the R161Q and R161G CblC mutants display lower protein stability and decreased dealkylation but not decyanation activity, suggesting that cyanocobalamin might be therapeutically useful for patients carrying mutations at Arg-161. The mutant proteins also exhibit impaired glutathione binding. In the presence of physiologically relevant glutathione concentrations, stabilization of the cob(II)alamin derivative is observed, which occurs at the expense of increased oxidation of glutathione. Futile redox cycling, which is suppressed in wild-type human CblC, explains the reported increase in oxidative stress levels associated with the CblC disorder.

Mammals utilize B_{12} or cobalamin derivatives as cofactors for two enzymes, methionine synthase and methylmalonyl-CoA mutase (1). Methionine synthase is essential for freeing the circulating form of the vitamin, 5-methyltetrahydrofolate, to the reduced folate pool, which in turn is needed to support various synthetic reactions necessary for cellular proliferation and homeostasis. Methylmalonyl-CoA mutase is a clearing house for methylmalonyl-CoA generated during breakdown of cholesterol, branched-chain amino acids, and odd-chain fatty acids, and it converts it to succinyl-CoA, which supports energy metabolism (2). Because mammals lack the ability to synthesize cobalamins *de novo*, they have evolved strategies to assimilate dietary B_{12} into the two biologically active cofactor forms, methylcobalamin (MeCbl)[2] and 5′-deoxyadenosylcobalamin (AdoCbl) (3–5). Insights into the complex pathway for transport and intracellular processing of B_{12} have emerged from clinical genetics studies on patients exhibiting derangements in cobalamin metabolism and biochemical studies on the affected proteins (3–6). Cobalamin disorders are classified into nine distinct complementation groups: *cbl*A–G, *cbl*J, and *mut* (5). In addition, an X-linked cobalamin disorder (*cbl*X) has been reported in which mutations localize to a transcriptional coregulator of the CblC gene (7).

Mutations in CblC (also referred to as MMACHC for methylmalonic aciduria type C and homocystinuria) represent the most common inborn error of cobalamin metabolism. Cobalamin disorders (OMIM 277400) are rare and inherited in an autosomal recessive manner (6). Heterogeneity within *cbl*C patients has been observed, and the most severe presentation of the multisystemic disease is associated with its early onset with affected individuals displaying neurologic, hematologic, and ophthalmologic abnormalities in the first years of life (8–10). The late onset form of the *cbl*C disorder has been reported in a smaller number of cases and is associated with a better response to treatment (10). So far, >75 mutations have been identified in the gene encoding CblC, and >700 affected alleles have been sequenced (8, 11, 12).

Human CblC exhibits relaxed substrate specificity and binds a variety of B_{12} derivatives (13). The structure of human CblC (14) reveals a commodious binding site for cobalamin where a variety of upper or β-axial ligands can be accommodated including cyano- (15), aquo-, methyl-, and 5′-deoxyadenosine (13, 16) in addition to a variety of unnatural cobalamins (16, 17). The substrate ambiguity of CblC is consistent with its varied processing functions following receipt of the B_{12} cargo from the lysosomal transporters, LMBD1 and ABCD4 (18, 19). Functionally, CblC catalyzes the removal of the upper or β-axial

* This work was supported by National Institutes of Health Grant DK45776 (to R. B.).

[1] To whom correspondence should be addressed: 4220C MSRB III, 1150 W. Medical Center Dr., University of Michigan, Ann Arbor, MI 48109-0600. Tel: 734-615-5238; E-mail: rbanerje@umich.edu.

[2] The abbreviations used are: MeCbl, methylcobalamin; AdoCbl, 5′-deoxyadenosylcobalamin; CNCbl, cyanocobalamin; GSCbl, glutathionyl-cobalamin; OH_2Cbl, aquocobalamin; ROS, reactive oxygen species.

ligand to generate a common intermediate that can be partitioned into the synthesis of the active cofactors, MeCbl and AdoCbl. When CblC binds CNCbl, electron transfer from reduced flavin, which is free or bound to an oxidoreductase (14, 15, 20), or from GSH (21) facilitates cleavage of the cobalt-carbon bond and elimination of the cyanide ion. In contrast, when CblC binds alkylcobalamins, it catalyzes the nucleophilic displacement of the alkyl group by a tightly bound GSH (16). The products of the decyanation and dealkylation reactions are cob(II)alamin and cob(I)alamin, respectively. Both are subsequently oxidized under aerobic conditions, to aquocobalamin (OH_2Cbl) (22). When CblC binds glutathionylcobalamin (GSCbl), it catalyzes the elimination of the glutathionyl group by GSH, forming GSSG (23).

The three-dimensional structure of CblC in the apo-, MeCbl- and AdoCbl-bound forms reveals the repurposing of a scaffold from the nitroreductase superfamily for housing the decyanation and dealkylation reactions (14, 24). Arginine residues frame the cavity around the upper axial face of the corrin ring, and Arg-161 and Arg-230 have been proposed to be important for GSH binding (Fig. 1, *A* and B) (24). Arg-161 is a highly conserved residue and does not make direct contact with the B_{12} cofactor in any of the available CblC structures. On the other hand, Arg-161 is involved in electrostatic interactions with citrate, a putative proxy for GSH that was co-crystallized in the CblC structure with AdoCbl bound (24). Mutations at Arg-161 are among the most common of the missense mutations leading to the *cblC* disorder, and depending on the nature of the substitution, these mutations are associated with either early (R161G) or late (R161Q) onset of the disease (20). The R161Q mutant has been characterized minimally, reported to decrease the T_m of CblC by 2 °C (25) and the MeCbl dealkylation activity ~10-fold (24).

In this study, we describe the detailed characterization of a pair of disease-associated mutations at Arg-161. Our study demonstrates weakened GSH binding and unexpectedly, stabilization of cob(II)alamin under aerobic conditions, which is accompanied by enhanced GSSG production. Characterization of the Arg-161 mutants reveals a latent mechanism for protecting against reactive oxygen species (ROS) production by wild-type human CblC by stabilizing OH_2Cbl. Corruption of this protective strategy by the Arg-161 mutations promotes futile redox cycling at physiologically relevant concentrations of GSH, between oxidized and reduced cobalamins, and leads to enhanced generation of ROS, a hallmark of the *cblC* disease (26).

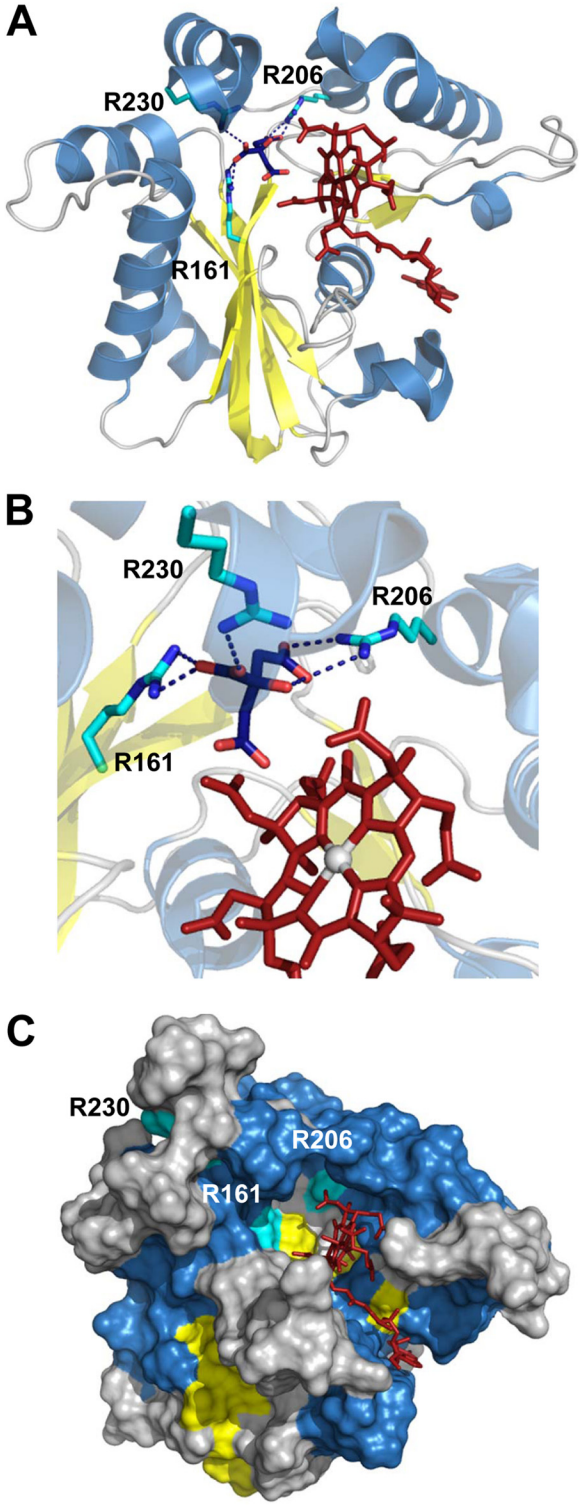

FIGURE 1. **Structure of human CblC with AdoCbl bound (Protein Data Bank (PDB) 3SOM) showing the locations of Arg-161, Arg-206 and Arg-230 predicted to be involved in GSH-binding.** *A*, cartoon representation of CblC structure (PDB: 3SOM) with helixes, β-sheets, and loops colored in *blue*, *yellow*, and *gray*, respectively. AdoCbl is shown in stick representation in *red*, and Arg-161, Arg-206, and Arg-230 are shown in *cyan*. Citrate bound to the active site is represented in *blue*. *B*, close-up of the hydrogen-bonding interactions between Arg-161, Arg-206, and Arg-230 and citrate bound at the active site. *C*, surface representation of the CblC structure indicating accessibility of the upper and lower faces of the corrin ring in the absence of bound GSH.

EXPERIMENTAL PROCEDURES

Materials—AdoCbl, CNCbl, OH_2Cbl, MeCbl, GSH, and NADPH were purchased from Sigma-Aldrich. Isopropyl β-D-thiogalactopyranoside, DL-DTT, and Tris (2-carboxyethyl) phosphine hydrochloride were from Gold Biotechnology. All other chemicals and reagents were purchased from Fisher Scientific unless otherwise stated.

Generation of Arg-161 Mutants of Human CblC—Construction of the mutants was performed using the QuikChange site-directed mutagenesis kit according to the manufacturer's instructions (Agilent Technologies Inc.). The pet28b vector

encoding the human CblC spanning residues 1–244 was used as a template with the following sense primers for generating R161G and R161Q, respectively: 5′-GGCTGGTTTGCCATCGGAGGGGTAGTGCGCTG-3′ and 5′-GGCTGGTTTGCCATCCAAGGGTAGTGCTGCTG-3′. The mutagenic codons specifying glycine and glutamine are underlined. The presence of the mutations was confirmed by nucleotide sequencing at the University of Michigan DNA Sequencing Core.

Expression and Purification of Wild-type and R161Q/G CblC—Recombinant wild-type and mutant CblC were expressed in *Escherichia coli* BL21(DE3) as described previously with minor modifications (14). Briefly, cells harvested from 6 liters of Luria Bertani medium were suspended in 150 ml of 50 mM Tris, pH 8.0, 300 mM NaCl, 20 mM imidazole containing 0.2 mg ml^{-1} lysozyme and one Complete EDTA-free protease inhibitor tablet. Cell lysates were cleared of debris by centrifugation (38,000 × *g* for 60 min), and CblC was isolated by affinity chromatography using a Ni-nitrilotriacetic acid-agarose column (Qiagen). The protein was further purified by size-exclusion chromatography using a HiLoad 16/60 Superdex 200 prep grade column (GE Healthcare) pre-equilibrated with 0.1 M HEPES, pH 7.4, 150 mM KCl, 10% glycerol (Buffer A). Fractions containing highly pure wild-type and mutant CblC were concentrated using Centricon filters (YM-10), flash-frozen in liquid nitrogen, and stored at −80 °C.

Thermal Denaturation Assays—The stability of R161G and R161Q relative to wild-type CblC was assessed in thermal denaturation experiments as described (14). Briefly, 0.5 mg ml^{-1} wild-type or R161Q/G CblC in Buffer A was incubated in a cuvette, and the temperature was gradually increased from 25 to 75 °C. The change in optical density at 600 nm was recorded in a spectrophotometer equipped with a temperature-controlled water bath (Fisher Scientific). The T_m was determined using Equation 1.

$$f = a/(1 + \exp(-(x - T_m)/b)) \quad \text{(Eq. 1)}$$

Dealkylation and Decyanation Activities of Wild-type and R161Q/G CblC—Dealkylation assays were performed in Buffer A at 25 °C and monitored by UV-visible spectroscopy. Reactions were initiated by the addition of GSH (1 μM–10 mM) to the aerobic assay mixtures (200 μl final volume) containing 30 μM CblC (wild type or R161Q/G) and 25 μM MeCbl, respectively. Kinetic parameters for the GSH-dependent dealkylation (k_{obs}, K_{act}) were determined from the dependence of the reaction rate on GSH concentration at 355 nm (corresponding to OH_2Cbl formation). Decyanation of CNCbl was monitored at 530 and 475 nm as described previously (15). Briefly, an anaerobic mixture of methionine synthase reductase (4 μM) was reduced with NADPH (200 μM), and the absorbance baseline was adjusted after 5 min of incubation. The decyanation reaction was initiated by the addition of a mixture containing 50 μM CblC and 20 μM CNCbl in Buffer A (200 μl final volume). Spectra were recorded at 25 °C under anaerobic conditions on a Cary100 spectrophotometer equipped with a temperature-controlled water bath.

EPR Spectroscopy—Wild-type and mutant CblC samples were prepared aerobically for EPR spectroscopy. Samples containing 100 μM wild-type or R161Q/G CblC, 75 μM MeCbl, and 10 mM GSH in Buffer A were incubated at 25 °C for 10 min. Reaction mixtures were then transferred to EPR tubes and frozen in liquid nitrogen. A base-off cob(II)alamin reference sample was prepared by photolysis of 100 μM AdoCbl in 1% H_3PO_4 as described previously (27). EPR spectra were recorded on a Bruker EMX spectrometer (Bruker Corp.) equipped with an Oxford ITC4 temperature controller, a Bruker gaussmeter, and a Hewlett-Packard model 5340 automatic frequency counter. The parameters used for spectral acquisition were: temperature, 100 K; microwave power, 20 milliwatt; microwave frequency, 9.38 GHz; receiver gain, 1×10^5; modulation amplitude, 10.0 G; modulation frequency, 100 kHz.

GSH-dependent Reduction of CblC-bound OH_2Cbl—OH_2Cbl (20 μM) was incubated with wild-type or R161Q/G CblC (50 μM) in Buffer A, and unbound OH_2Cbl was removed using a Microcon YM-10 centrifugal filtration unit. Then, 10 mM GSH was added to initiate the reduction reaction. The rate of OH_2Cbl reduction was determined by the increase in absorbance at 475 nm due to cob(II)alamin formation at 25 °C.

HPLC Analysis of GSH and GSSG—The concentrations of GSH and GSSG in assay mixtures were determined at the start and end of the OH_2Cbl reduction reactions using an HPLC method as described (21, 28). Briefly, OH_2Cbl (20 μM) bound to wild-type, R161Q, and R161G CblC proteins (50 μM) was treated with 10 mM GSH, and the reaction was allowed to proceed at 25 °C for 1 h. Proteins were precipitated using 1:1 (v/v) 0.21 M metaphosphoric acid solution containing 5.3 mM EDTA and 150 mM NaCl, and thiols in the supernatant were alkylated with monoiodoacetic acid (37 mM final concentration). Then, the pH of the samples was adjusted to ~8 by the addition of 3 μl of saturated K_2CO_3, and the samples were incubated for 1 h at room temperature in the dark. The samples were further derivatized by the addition of an equal volume of 2,4-dinitrofluorobenzene (1.5% v/v in ethanol) to the reaction mixture, and the reaction was allowed to proceed for 4 h at room temperature in the dark. The derivatized GSH and GSSG samples were separated by HPLC on a μBondapak NH_2 column (Waters, 300 × 3.9 mm, 10 μm) using an 18–60% (v/v) gradient of Solvent B with a flow rate of 1 ml min^{-1}. Solvent A contained 80% (v/v) methanol, and Solvent B contained 1.25 M ammonium acetate, 25% acetic acid, and 50% methanol. Under these conditions, the retention times for GSH and GSSG were 17.4 and 22.5 min, respectively.

Oxygen Consumption Analysis—The rate of oxygen consumption accompanying GSH-dependent decyanation of CNCbl or reduction of OH_2Cbl by CblC was determined using a polarographic assay. The reaction mixture containing wild-type or mutant CblC (50 μM) and either CNCbl or OH_2Cbl (20 μM) in Buffer A was incubated with 10 mM GSH in a Gilson type chamber (1.5 ml total volume) equipped with a Clark oxygen electrode and a magnetic stirrer. Oxygen consumption was monitored at room temperature on a Kipp & Zonen BD single channel chart recorder in the absence or presence of GSH. Oxygen consumption was expressed as μmol of O_2 min^{-1} mg^{-1} protein at 22 °C.

Isothermal Titration Calorimetry (ITC)—Calorimetric studies were performed using a VP-ITC microcalorimeter (Micro-

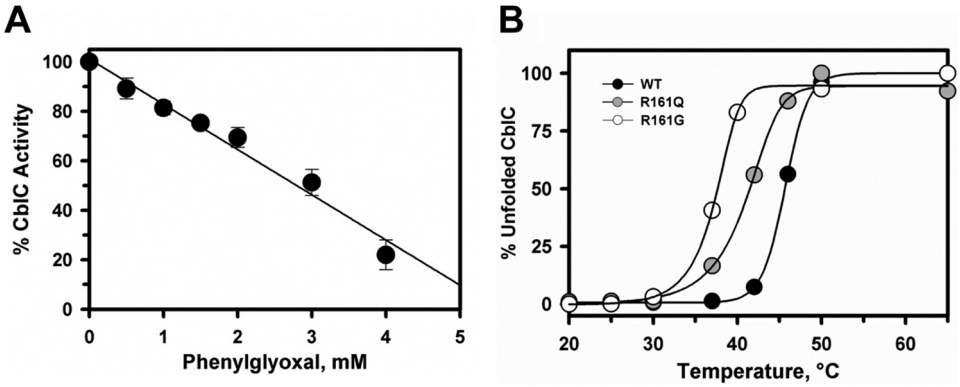

FIGURE 2. **Effect of arginines on the activity and stability of CblC.** *A*, phenylglyoxal inhibits dealkylation of MeCbl by CblC. CblC (30 μM) and MeCbl (20 μM) in Buffer A were incubated with 10 mM GSH and increasing concentrations of phenylglyoxal (0–4 mM) for 30 min, and its effect on the demethylation activity was determined as described under "Experimental Procedures." Plots were normalized to denote maximum activity in the absence of phenylglyoxal. The data represent the mean ± S.D. of three independent experiments. *B*, the effect of R161Q/G substitutions on the stability of CblC as monitored at 600 nm. Plots for the temperature-dependent unfolding of R161Q (*gray circles*) and R161G (*open circles*) mutants are compared with wild-type (*black circles*) CblC. The plots were normalized to the starting absorbance at 600 nm representing folded protein. The T_m values were determined as described under "Experimental Procedures."

Cal Inc., Northampton, MA). Binding of GSH (0.5–10 mM) to wild-type or mutant CblC (20–200 μM) was monitored at 25 °C in Buffer A by titrating aliquots from a 300-μl syringe loaded with the ligand into a 1.43-ml sample cell containing the protein. Samples were prepared by filtration through a 0.2-μm filter and then degassed under vacuum at 4 °C using a ThermoVac sample degasser. GSH (10-μl injections of 5 μM GSH for wild type and 50 μM GSH for the Arg-161 mutants) was added to 20–35 μM CblC. The data were analyzed using a single-site binding model using the MicroCal ORIGIN program. Titrations were performed in triplicate.

RESULTS

Role of Arginines in CblC—Arginine residues lining the active site of CblC have been suggested to be involved in GSH binding (24). To test this hypothesis, we used phenylglyoxal, an arginine-reactive reagent (29). Incubation of CblC with 4 mM phenylglyoxal at 37 °C resulted in ~80% inhibition of the GSH-dependent MeCbl dealkylation in 30 min (Fig. 2*A*). Higher phenylglyoxal concentrations induced protein precipitation.

Relative Stabilities of R161Q and R161G CblC—As the nature of the substitution at Arg-161 dictates early (R161G) *versus* late (R161Q) onset of the *cblC* disease, we determined the impact of these mutations on protein stability (Fig. 2*B*). Comparison of the thermal denaturation profiles demonstrated that the R161G mutant is considerably less stable (T_m = 38.1 ± 0.7 °C) than wild-type CblC (T_m = 46.6 ± 1.5 °C), whereas R161Q showed intermediate stability (T_m = 43.4 ± 0.2 °C).

Effect of the R161G/Q Mutants on the Dealkylation Activity of CblC—The alkyltransferase activities of R161Q and R161G CblC were tested in the presence of MeCbl and 1 mM GSH (Fig. 3, *A–C*). Both mutants exhibited diminished activity: ~6-fold (R161Q) and 10-fold (R161G) lower than wild-type CblC (Fig. 3*D*). The dependence of the k_{obs} of the demethylase activity on GSH concentration was determined under aerobic conditions yielding a K_{act} for GSH = 0.025 ± 0.004 mM (wild-type CblC), 1.03 ± 0.09 mM (R161Q CblC), and 0.62 ± 0.07 mM (R161G CblC), respectively (Fig. 3, *E* and *F*). Thus, the Arg-161 mutants exhibit a 25–40-fold reduced affinity for GSH as compared with wild-type CblC.

Stabilization of Cob(II)alamin by the Arg-161 CblC Mutants—Because GSH concentrations can vary from 1 to 10 mM depending on the cell type (30, 31), the reduced affinity of the CblC mutants for GSH could be masked. Hence, we decided to examine the dealkylation reaction at higher GSH concentrations. Surprisingly, in the presence of 5–10 mM GSH, cob(I-I)alamin rather than OH_2Cbl was observed as evidenced by the increase in absorption at 473 nm (Fig. 4*A*). Stabilization of the cob(II)alamin species by CblC is unexpected because wild-type CblC stabilizes cob(III)alamin with a water ligand, *i.e.* OH_2Cbl (16), even in the presence of 10 mM GSH (Fig. 4*B*). Under anaerobic conditions, the cob(I)alamin product of the dealkylation reaction was observed with the R161Q/G mutants consistent with nucleophilic displacement of the methyl group of MeCbl by the thiolate of GSH (data not shown) as reported previously for wild-type CblC (16). Further evidence for stabilization of the paramagnetic cob(II)alamin species by the mutants was obtained by EPR spectroscopy (Fig. 4*C*). The product of R161G/Q-catalyzed dealkylation of MeCbl under aerobic conditions was clearly base-off cob(II)alamin. Base-off refers to the conformation of cobalamin in which the endogenous dimethylbenzimidazole base, which is a component of the corrin ring structure, is not coordinated to the cobalt. The eight-line hyperfine splitting and the 140 Gauss spacing between the singlets in the high-field region of the EPR spectra are also seen in the spectrum of authentic base-off cobalamin (Fig. 4*C*, *lower spectrum*). The eight-line hyperfine splitting arises from coupling of the unpaired electron with the cobalt nucleus (I = 7/2).

Effect of the R161G/Q Mutants on the Decyanation Activity of CblC—Decyanation of CNCbl by R161Q and R161G CblC was monitored anaerobically in the presence of NADPH/methionine synthase reductase (Fig. 5). In contrast to the 6–10-fold effects on dealkylation activity and as reported previously for the R161Q mutant (20), a negligible effect of the mutations was observed on the decyanation activity. The k_{obs} values for R161Q and R161G were 0.11 ± 0.01 and 0.12 ± 0.01 min^{-1}, respec-

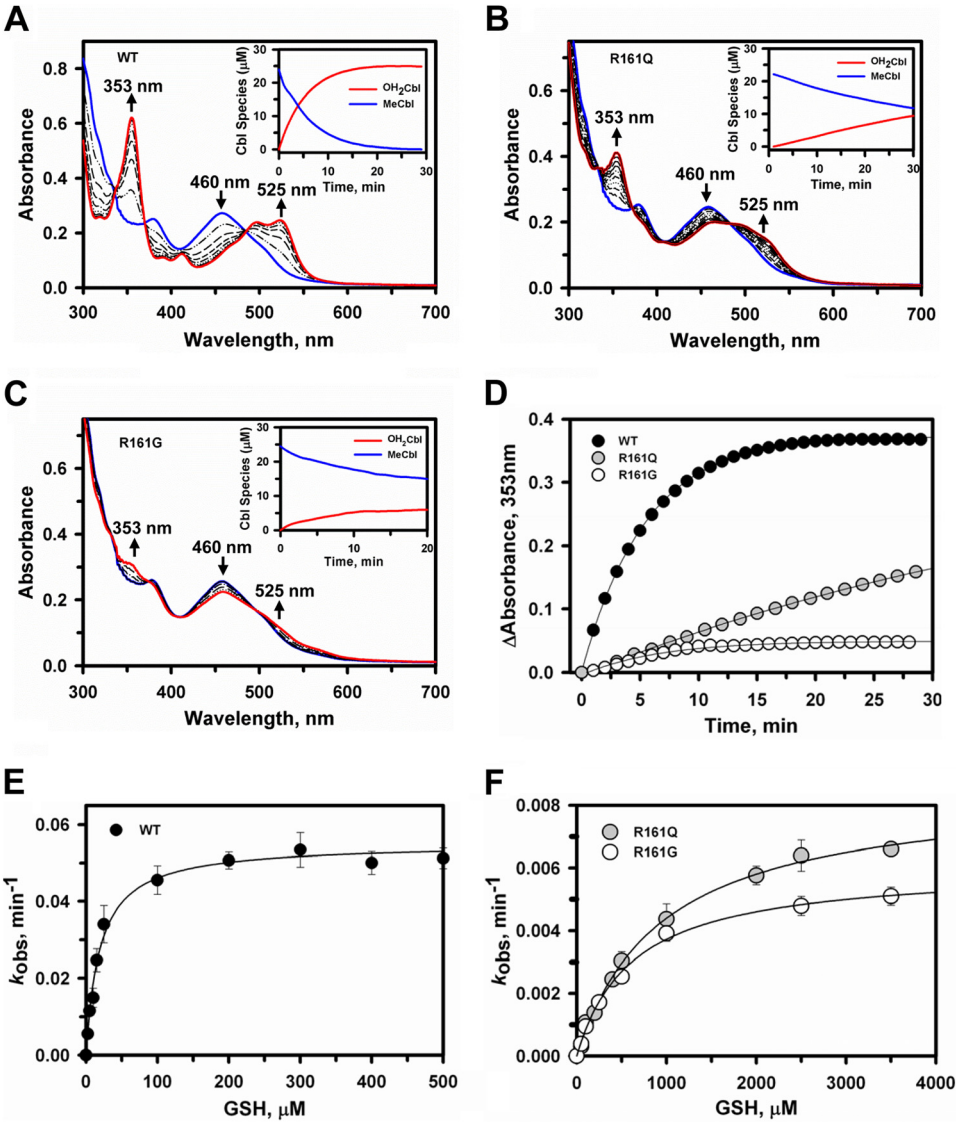

FIGURE 3. **Dealkylation of MeCbl by wild-type and R161Q/G CblC.** *A–C*, time-dependent changes in the UV-visible absorption spectra of MeCbl (25 μM) bound to wild-type (*A*), R161Q (*B*), or R161G (*C*) CblC (30 μM) in Buffer A following the addition of 1 mM GSH under aerobic conditions, at 25 °C. The initial CblC-bound MeCbl spectrum has an absorption maxima at 460 nm (*blue trace*), whereas the product spectra recorded at 30 min shows features characteristic for OH_2Cbl at 353 and 525 nm (*red traces*). The *insets* in in *A–C* show the concentration of the MeCbl consumed and OH_2Cbl formed during the reactions. *D*, comparison of the MeCbl dealkylation rates for wild-type (*black circles*), R161Q (*gray circles*), and R161G CblC (*open circles*). *E* and *F*, dependence of the initial rate of dealkylation of MeCbl bound to wild-type (*E*) or R161Q/G (*F*) CblC on GSH concentration. Aerobic reaction mixtures containing 30 μM CblC, 25 μM MeCbl, and 0–5 mM GSH in Buffer A were monitored at 25 °C at 353 nm. The data are the mean ± S.D. of at least three independent experiments.

tively, which is comparable with the value for wild-type CblC (0.13 ± 0.01 min^{-1}).

Reduction of CblC-bound OH_2Cbl by GSH—The kinetics of GSH-dependent reduction of OH_2Cbl bound to wild-type CblC *versus* R161Q/G CblC were compared. In the presence of 10 mM GSH, cob(II)alamin formation was observed under both aerobic (Fig. 6*A*) and anaerobic (Fig. 6*B*) conditions with the R161Q/G mutants. In contrast, the addition of 10 mM GSH to wild-type CblC with bound OH_2Cbl induced spectral changes consistent with base-off OH_2Cbl, but detectable cob(II)alamin was only observed under anaerobic conditions (not shown). The kinetics of cob(II)alamin appearance were monitored at 475 nm and yielded k_{obs} values of 0.0046 ± 0.0005 and 0.027 ± 0.003 min^{-1} for the R161Q and R161G mutants, respectively (Fig. 6*A*, *inset*). Under anaerobic conditions, the k_{obs} for cob(II)alamin formation by wild-type, R161Q, and R161G CblC were 0.015 ± 0.002, 0.017 ± 0.002, and 0.018 ± 0.003 min^{-1}, respectively (Fig. 6*B* and *inset*). GSSG generation was enhanced in the presence of R161Q (0.9 ± 0.1 mM in 60 min) and R161G (1.9 ± 0.2 mM) CblC as compared with wild-type (0.47 ± 0.04 mM) CblC (Fig. 6*C*). The kinetics of oxygen consumption paralleled the difference in GSSG accumulation by the wild type *versus* the Arg-161 mutants (Fig. 6*D*).

DISCUSSION

The repurposing of the nitroreductase scaffold during evolution gave rise to CblC, an enzyme that exhibits substrate ambiguity and impressive catalytic versatility. The structures of two recently described cobalamin-dependent dehalogenases reveal that within the nitroreductase superfamily, they most closely resemble CblC (32, 33), suggesting that the ancestry of CblC, described thus far only in higher organisms, is related to these

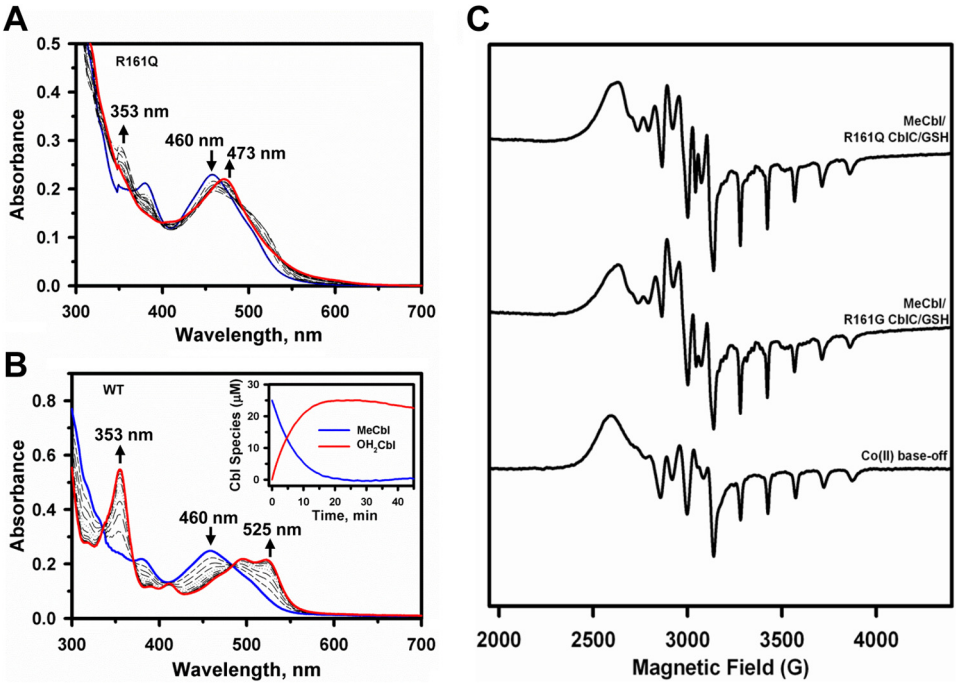

FIGURE 4. **Stabilization of cob(II)alamin by R161Q/G CblC at high GSH concentrations.** UV-visible spectra were recorded to monitor dealkylation of MeCbl. *A* and *B*, the reaction mixtures contained R161Q CblC (*A*) or wild-type CblC (30 μM) and MeCbl (25 μM) (*B*) in aerobic Buffer A at 25 °C. The initial spectra are shown in *blue*, and spectra were recorded every 3 min following the addition of 10 mM GSH (only a few spectra are shown for clarity). The spectral changes were consistent with formation of cob(II)alamin with an absorption maximum at 473 nm with R161Q CblC (*red trace*, A) and OH_2Cbl with absorption maxima at 353 and 525 nm with wild-type CblC (*red trace*, B). *C*, EPR spectra of authentic cob(II)alamin (*lower*) generated as described under "Experimental Procedures" compared with cob(II)alamin formed during dealkylation of MeCbl catalyzed by R161Q (*upper*) and R161G (*middle*) CblC. The samples were prepared as described under "Experimental Procedures."

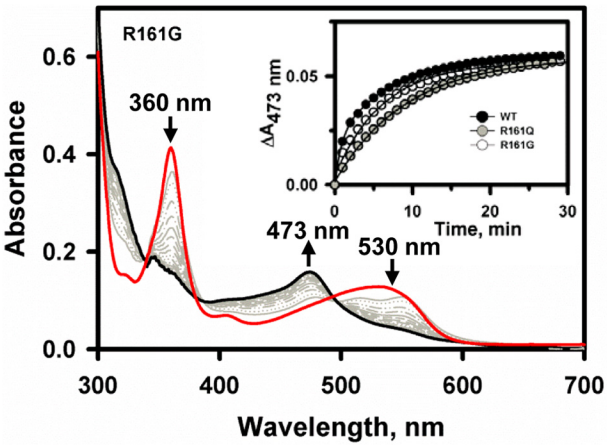

FIGURE 5. **Decyanation kinetics of wild-type and mutant CblCs.** Shown are changes in the UV-visible absorption spectrum of CNCbl (20 μM) bound to R161G CblC (50 μM) in Buffer A at 25 °C following addition to a mixture of methionine synthase reductase/NADPH (4 μM/200 μM) under anaerobic conditions. The initial spectrum is in *red*, selected traces over the reaction course are in *gray*, and the final spectrum at 60 min is in *black*. The *inset* shows the reaction kinetics monitored at 473 nm for wild-type (*black circles*), R161Q (*gray circles*), and R161G (*open circles*) CblC.

bacterial dehalogenases. The broad range of catalytic functions exhibited by CblC includes decyanation, dealkylation, and OH_2Cbl reduction (15, 16, 21). The structure of human CblC shows a cavernous active site (14, 24), which can accommodate cobalamins with a variety of upper axial ligands (13). Cobalamin is bound in a base-off conformation, and the lower or α-face of the corrin ring is vacant and solvent-accessible in the structure of human CblC (14, 24). Unlike the *Caenorhabditis elegans* CblC, cob(I)alamin and cob(II)alamin bound to wild-type human CblC are subject to facile oxidation forming OH_2Cbl (Fig. 7). The structure of human CblC suggests that access to oxidants could occur from the upper or lower axial face of cobalamin (Fig. 1*C*).

The ability of CblC to displace the glutathionyl moiety of GSCbl with GSH (21, 23) indicates that the active site can accommodate two equivalents of GSH. Although a structure of CblC with GSH has been elusive, the binding site for one of the GSH moieties is suggested by the active site location of citrate, derived from the crystallization solution (24). Multiple electrostatic interactions pin the citrate in the arginine-rich pocket on the upper face of the corrin ring, and these interactions include Arg-161 (Fig. 1*B*). An arginine residue is also involved in GSH binding in some glutathione *S*-transferase superfamily members (34), and their mutation affects catalytic activity (35–37).

Modulation of CblC activity by Arg-161 is of interest because it is a common locus for missense mutations in patients with the *cblC* class of cobalamin defects (9). Arg-161 is highly conserved, and disease severity and age of onset are correlated with whether it is mutated to glutamine or glycine. Furthermore, *cblC* patients exhibit high levels of oxidative damage biomarkers, and human *cblC* fibroblasts have elevated levels of ROS (26, 38). Furthermore, an imbalance in GSH metabolism with a significant decrease in GSH and an increase in GSSG concentration has been reported in CblC-deficient individuals (40). Although limited qualitative analyses of R161Q CblC have revealed impaired GSH-dependent MeCbl dealkylation activity (24), they have not provided insights into elevated ROS forma-

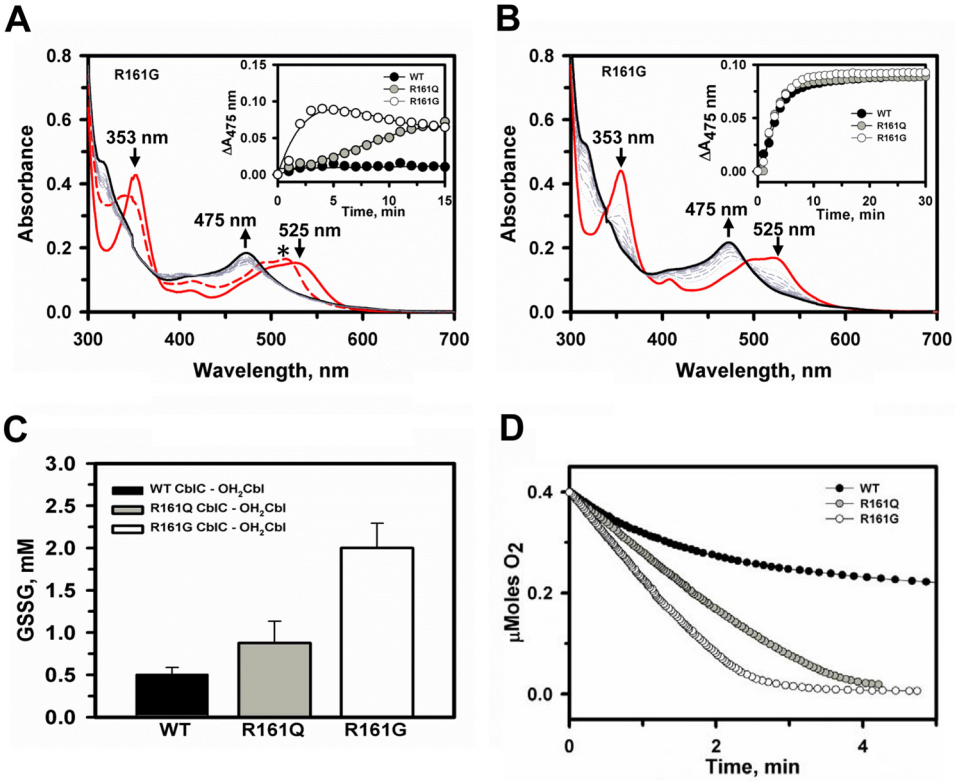

FIGURE 6. **GSH-dependent reduction of OH_2Cbl by wild-type and R161Q/G CblC.** *A* and *B*, changes in the UV-visible absorption spectra of OH_2Cbl (20 μM) bound to R161G CblC (50 μM) in Buffer A were monitored at 25 °C under aerobic (*A*) and anaerobic conditions (*B*). Reactions were initiated by the addition of 10 mM GSH. The initial spectra are in *red*, selected traces over the reaction course time are in *gray*, and the final spectra at 60 min are in *black*. Following the addition of GSH to the aerobic sample (*A*), the absorption maximum shifts from 525 to 516 nm (*red dashed trace*) before cob(II)alamin formation (473 nm maximum) is observed. The *insets* in *A* and *B* show the reaction kinetics monitored at 475 nm for wild-type (*black circles*), R161Q (*gray circles*), and R161G (*open circles*) CblC. The slight decrease in absorbance at 475 nm over time observed with the more active R161G CblC suggests slow oxidation of cob(II)alamin to OH_2Cbl. *C*, HPLC analysis of GSSG formed after 60 min in the assay mixtures during the reaction shown in *A*. The data represent the mean ± S.D. of three independent experiments. *D*, oxygen consumption kinetics associated with GSH-dependent reduction of OH_2Cbl in the presence of wild-type (*black circles*), R161Q (*gray circles*), and R161G (*open circles*) CblC.

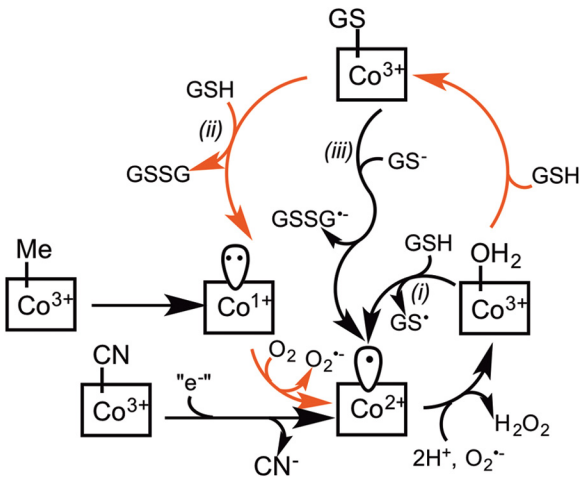

FIGURE 7. **Alternative mechanisms for redox cycling and cob(II)alamin stabilization by the R161Q/G mutants.** Demethylation of MeCbl by CblC leads to cob(I)alamin formation, which is labile and is readily oxidized to form cob(II)alamin, and subsequently, to OH_2Cbl, which is stabilized by wild-type CblC. Enhanced formation of GSSG accompanying cob(II)alamin stabilization by the R161 mutants could occur by one of three routes denoted *i–iii*. In path i, OH_2Cbl is reduced by GSH to cob(II)alamin. In paths ii and iii, OH_2Cbl is initially converted to GSCbl. The latter is either displaced by a second mole of GSH (path ii) or reduced, leading to cob(II)alamin (path iii). The $GS^{\bullet}$ radical formed in path i is rapidly quenched by GSH, giving $GSSG^{\bullet-}$, which is also formed in path iii, and the $GSSG^{\bullet-}$ radical reacts rapidly with O_2 to form $O_2^{\bullet-}$, further enhancing ROS production. The reactions that are predicted to be accelerated in the Arg-161 mutants are depicted by *red arrows*.

tion nor the phenotypic differences associated with a glycine *versus* glutamine substitution at this location.

In this study, we report that mutations at Arg-161 are destabilizing and reduce the T_m of CblC by ~3 °C (R161Q) and 8.5 °C (R161G), respectively, as compared with the wild-type protein (Fig. 2*B*). With a T_m of 38.1 ± 0.7 °C, the R161G mutant would be very susceptible to aggregation at the normal body temperature of 37 °C, which is highly likely to be a contributing factor to early disease onset. Mutations at Arg-161 also decrease the affinity of CblC for GSH by 25- (R161G) and 40-fold (R161Q), respectively, consistent with a role for this residue in substrate binding, as postulated (24). The k_{obs} of the MeCbl dealkylation reaction is diminished 6–10-fold by the R161Q and R161G mutations (Fig. 3). Interestingly, and in contrast to the dealkylation activity of CblC, the Arg-161 mutants do not significantly affect the decyanation activity in the presence of NADPH and the flavoprotein, methionine synthase reductase (Fig. 5). These results suggest that unlike a number of *cblC* patients who do not respond well to CNCbl (or vitamin B_{12}) therapy (41, 42), patients carrying the R161Q/G mutants might. Given their lower T_m values, however, the efficacy of CNCbl therapy would be predicated by the steady-state levels of the R161Q/G mutants.

Unexpectedly, the R161Q and R161G mutations stabilize cob(II)alamin in the presence of high but not low GSH and are

thereby distinct from wild-type CblC, which stabilizes OH_2Cbl (Figs. 3 and 4) and binds it with higher affinity. Depending on the cell type, both 1 mM GSH and 10 mM GSH concentrations are physiologically relevant. The preferential stabilization by the Arg-161 mutants of cob(II)alamin with a concomitant increase in GSSG production offers insights into ROS production, which is relevant to disease (38, 39).

In the dealkylation and decyanation reactions catalyzed by wild-type human CblC, the initially formed cob(I)alamin and cob(II)alamin products are oxidized to OH_2Cbl (Fig. 7). Although the electron acceptors during each of these oxidation reactions are not known, it is presumably O_2 during oxidation of cob(I)alamin and the superoxide anion ($O_2^{\cdot-}$) during oxidation of cob(II)alamin based on thermodynamic considerations. Thus, the redox potentials for the $O_2/O_2^{\cdot-}$ and $O_2^{\cdot-}/H_2O_2$ couples at pH 7.0 are −330 mV and +890 mV, respectively (43). The redox potentials for the base-off cob(II)alamin/cob(I)alamin and base-off OH_2Cbl/cob(II)alamin couples are −500 mV and +510 mV, respectively (44). In solution, cob(II)alamin is an efficient $O_2^{\cdot-}$ scavenger, reacting at rates approaching that of superoxide dismutase (45). The accessibility of the upper axial face of the corrin ring to oxidants is not known because a structure of CblC with GSH is not available. The lower axial corrin face appears to be solvent-exposed (Fig. 1*C*), allowing access to oxidants. In principle, the Arg-161 mutants could stabilize cob(II)alamin by limiting access of oxidant to the cobalt or by increasing futile redox cycling. The observed formation of GSSG under aerobic conditions where cob(II)alamin is apparently stabilized is indicative of cryptic cycling of cobalt between the 2+ and 3+ oxidation states (Fig. 7).

Stabilization of cob(II)alamin and oxidation of GSH to GSSG has been observed previously with the *C. elegans* CblC (21) and occurs via a futile redox cycle (Fig. 7), which is suppressed in human CblC. OH_2Cbl-dependent oxidation of thiols to their disulfides in solution has been reported previously (46–48). In principle, the redox cycle could proceed via one of three pathways. In the first, OH_2Cbl is reduced by GSH to form cob(II)alamin, and the resulting thiyl radical is rapidly quenched in reactions with a second mole of GSH and O_2 to give GSSG and $O_2^{\cdot-}$. The redox potential for the $GS^{\cdot}$/GSH couple is +920 mV at pH 7.4 (49) and considerably more positive than for the base-off OH_2Cbl/cob(II)alamin couple (+510 mV). Kinetic coupling of the unfavorable GSH oxidation reaction to formation of $GSSG^{\cdot-}$ from $GS^{\cdot}$ and GSH followed by quenching of the radical anion with oxygen could conceivably provide the driving force for this reaction.

In the second pathway, OH_2Cbl is converted to GSCbl, but only at high concentrations of GSH, and the resulting GSCbl is cleaved by GSH in a nucleophilic displacement reaction to yield GSSG. The product of this reaction is the highly reactive cob(I)alamin species, which reacts rapidly with O_2 to form cob(II)alamin and $O_2^{\cdot-}$. It is possible that mutation of the Arg-161 residue results in poorer stabilization of $O_2^{\cdot-}$, promoting its loss from the active site and thus contributing to the stabilization of cob(II)alamin. Stabilization of $O_2^{\cdot-}$ produced *in situ* via autoxidation has been observed in the heme pocket in the β-chain of hemoglobin (50). Path ii invokes binding of a second equivalent of GSH to CblC (Fig. 7). We know that the first equivalent of GSH binds tightly to human CblC ($K_D = 30 \pm 1\ \mu$M (16)) and is positioned to promote nucleophilic chemistry and to suppress sulfur coordination to the cobalt because conversion of wild-type CblC-bound OH_2Cbl to GSCbl is not observed (21, 22). Stabilization of cob(II)alamin at high GSH concentrations suggests unmasking of a second lower affinity GSH binding site by mutations at the Arg-161 position. Accommodation of two GSH equivalents in the active site is consistent with the conversion of GSCbl to cob(I)alamin in the presence of GSH by bovine and *C. elegans* CblC (21, 23). In the third pathway, electron transfer from the second equivalent of GSH yields cob(II)alamin and $GSSG^{\cdot-}$. This third mechanism is supported by solution studies demonstrating reduction of thiolate-liganded cob(III)alamin to cob(II)alamin by a peripherally bound thiol, presumed to be present at the lower axial corrin face (39).

CONCLUSION

We demonstrate that at physiologically relevant GSH concentrations, cob(II)alamin is the predominant species bound to CblC in patients harboring the R161G and R161Q mutations. Both mutations decrease the T_m of CblC, and the differences in the magnitude of destabilization likely contribute to early *versus* late onset of the disease. Furthermore, we show that the mutations impair the dealkylation but not the decyanation activity of CblC, suggesting that in patients with mutations at Arg-161, CNCbl might be therapeutically useful. Finally, based on precedence for deglutathionylation of GSCbl by GSH, we favor path ii as an explanation for how the Arg-161 mutants stabilize cob(II)alamin. We predict that loss of the positively charged Arg-161 residue destabilizes $O_2^{\cdot-}$ binding in the corrin pocket and thus stabilizes cob(II)alamin against further oxidation. On the other hand, mutation of Arg-161 to the smaller glutamine and glycine residues promotes binding of a second equivalent of GSH, which forms a transient GSCbl species by displacing the water ligand in OH_2Cbl. Because GSCbl is not observed even at high concentrations of GSH, it suggests that its formation is slow, whereas its conversion to cob(II)alamin (via oxidation of the initially formed cob(I)alamin) is rapid. By promoting futile cycling, the Arg-161 mutants lead to enhanced $O_2^{\cdot-}$ and GSSG formation, contributing to oxidative stress observed in fibroblasts (26) and increased GSSG levels seen in lymphocytes from *cblC* patients (40).

REFERENCES

1. Banerjee, R., and Ragsdale, S. W. (2003) The many faces of vitamin B_{12}: catalysis by cobalamin-dependent enzymes. *Annu. Rev. Biochem.* **72,** 209–247
2. Banerjee, R. (2001) Radical peregrinations catalyzed by coenzyme B_{12}-dependent enzymes. *Biochemistry* **40,** 6191–6198
3. Banerjee, R., Gherasim, C., and Padovani, D. (2009) The tinker, tailor, soldier in intracellular B_{12} trafficking. *Curr. Opin. Chem. Biol.* **13,** 484–491
4. Gherasim, C., Lofgren, M., and Banerjee, R. (2013) Navigating the B_{12} road: assimilation, delivery and disorders of cobalamin. *J. Biol. Chem.* **288,** 13186–13193
5. Watkins, D., and Rosenblatt, D. S. (2012) Update and new concepts in vitamin responsive disorders of folate transport and metabolism. *J. Inherit. Metab. Dis.* **35,** 665–670
6. Shevell, M. I., and Rosenblatt, D. S. (1992) The neurology of cobalamin. *Can. J. Neurol. Sci.* **19,** 472–486

7. Yu, H. C., Sloan, J. L., Scharer, G., Brebner, A., Quintana, A. M., Achilly, N. P., Manoli, I., Coughlin, C. R., 2nd, Geiger, E. A., Schneck, U., Watkins, D., Suormala, T., Van Hove, J. L., Fowler, B., Baumgartner, M. R., Rosenblatt, D. S., Venditti, C. P., and Shaikh, T. H. (2013) An X-linked cobalamin disorder caused by mutations in transcriptional coregulator *HCFC1*. *Am. J. Hum. Genet.* **93,** 506–514
8. Lerner-Ellis, J. P., Tirone, J. C., Pawelek, P. D., Doré, C., Atkinson, J. L., Watkins, D., Morel, C. F., Fujiwara, T. M., Moras, E., Hosack, A. R., Dunbar, G. V., Antonicka, H., Forgetta, V., Dobson, C. M., Leclerc, D., Gravel, R. A., Shoubridge, E. A., Coulton, J. W., Lepage, P., Rommens, J. M., Morgan, K., and Rosenblatt, D. S. (2006) Identification of the gene responsible for methylmalonic aciduria and homocystinuria, cblC type. *Nat. Genet.* **38,** 93–100
9. Lerner-Ellis, J. P., Anastasio, N., Liu, J., Coelho, D., Suormala, T., Stucki, M., Loewy, A. D., Gurd, S., Grundberg, E., Morel, C. F., Watkins, D., Baumgartner, M. R., Pastinen, T., Rosenblatt, D. S., and Fowler, B. (2009) Spectrum of mutations in *MMACHC*, allelic expression, and evidence for genotype-phenotype correlations. *Hum. Mutat.* **30,** 1072–1081
10. Rosenblatt, D. S., Aspler, A. L., Shevell, M. I., Pletcher, B. A., Fenton, W. A., and Seashore, M. R. (1997) Clinical heterogeneity and prognosis in combined methylmalonic aciduria and homocystinuria (cblC). *J. Inherit. Metab. Dis.* **20,** 528–538
11. Liu, M. Y., Yang, Y. L., Chang, Y. C., Chiang, S. H., Lin, S. P., Han, L. S., Qi, Y., Hsiao, K. J., and Liu, T. T. (2010) Mutation spectrum of *MMACHC* in Chinese patients with combined methylmalonic aciduria and homocystinuria. *J. Hum. Genet.* **55,** 621–626
12. Gündüz, M., Ekici, F., Özaydın, E., Ceylaner, S., and Perez, B. (2014) Reversible pulmonary arterial hypertension in cobalamin-dependent cobalamin C disease due to a novel mutation in the *MMACHC* gene. *Eur. J. Pediatr.* **173,** 1707–1710
13. Hannibal, L., Kim, J., Brasch, N. E., Wang, S., Rosenblatt, D. S., Banerjee, R., and Jacobsen, D. W. (2009) Processing of alkylcobalamins in mammalian cells: a role for the MMACHC (*cblC*) gene product. *Mol. Genet. Metab.* **97,** 260–266
14. Koutmos, M., Gherasim, C., Smith, J. L., and Banerjee, R. (2011) Structural basis of multifunctionality in a vitamin B_{12}-processing enzyme. *J. Biol. Chem.* **286,** 29780–29787
15. Kim, J., Gherasim, C., and Banerjee, R. (2008) Decyanation of vitamin B_{12} by a trafficking chaperone. *Proc. Natl. Acad. Sci. U.S.A.* **105,** 14551–14554
16. Kim, J., Hannibal, L., Gherasim, C., Jacobsen, D. W., and Banerjee, R. (2009) A human vitamin B_{12} trafficking protein uses glutathione transferase activity for processing alkylcobalamins. *J. Biol. Chem.* **284,** 33418–33424
17. Ruetz, M., Gherasim, C., Gruber, K., Fedosov, S., Banerjee, R., and Kräutler, B. (2013) Access to organometallic arylcobaltcorrins through radical synthesis: 4-ethylphenylcobalamin, a potential "antivitamin B_{12}". *Angew. Chem. Int. Ed. Engl.* **52,** 2606–2610
18. Rutsch, F., Gailus, S., Miousse, I. R., Suormala, T., Sagné, C., Toliat, M. R., Nürnberg, G., Wittkampf, T., Buers, I., Sharifi, A., Stucki, M., Becker, C., Baumgartner, M., Robenek, H., Marquardt, T., Höhne, W., Gasnier, B., Rosenblatt, D. S., Fowler, B., and Nürnberg, P. (2009) Identification of a putative lysosomal cobalamin exporter altered in the cblF defect of vitamin B_{12} metabolism. *Nat. Genet.* **41,** 234–239
19. Coelho, D., Kim, J. C., Miousse, I. R., Fung, S., du Moulin, M., Buers, I., Suormala, T., Burda, P., Frapolli, M., Stucki, M., Nürnberg, P., Thiele, H., Robenek, H., Höhne, W., Longo, N., Pasquali, M., Mengel, E., Watkins, D., Shoubridge, E. A., Majewski, J., Rosenblatt, D. S., Fowler, B., Rutsch, F., and Baumgartner, M. R. (2012) Mutations in *ABCD4* cause a new inborn error of vitamin B_{12} metabolism. *Nat. Genet.* **44,** 1152–1155
20. Froese, D. S., Zhang, J., Healy, S., and Gravel, R. A. (2009) Mechanism of vitamin B_{12}-responsiveness in *cblC* methylmalonic aciduria with homocystinuria. *Mol. Genet. Metab.* **98,** 338–343
21. Li, Z., Gherasim, C., Lesniak, N. A., and Banerjee, R. (2014) Glutathione-dependent one-electron transfer reactions catalyzed by a B_{12} trafficking protein. *J. Biol. Chem.* **289,** 16487–16497
22. Jeong, J., Ha, T. S., and Kim, J. (2011) Protection of aquo/hydroxocobalamin from reduced glutathione by a B_{12} trafficking chaperone. *BMB Rep.* **44,** 170–175
23. Jeong, J., Park, J., Park, J., and Kim, J. (2014) Processing of glutathionylcobalamin by a bovine B_{12} trafficking chaperone bCblC involved in intracellular B_{12} metabolism. *Biochem. Biophys. Res. Commun.* **443,** 173–178
24. Froese, D. S., Krojer, T., Wu, X., Shrestha, R., Kiyani, W., von Delft, F., Gravel, R. A., Oppermann, U., and Yue, W. W. (2012) Structure of MMACHC reveals an arginine-rich pocket and a domain-swapped dimer for its B_{12} processing function. *Biochemistry* **51,** 5083–5090
25. Froese, D. S., Healy, S., McDonald, M., Kochan, G., Oppermann, U., Niesen, F. H., and Gravel, R. A. (2010) Thermolability of mutant MMACHC protein in the vitamin B_{12}-responsive *cblC* disorder. *Mol. Genet. Metab.* **100,** 29–36
26. Richard, E., Jorge-Finnigan, A., Garcia-Villoria, J., Merinero, B., Desviat, L. R., Gort, L., Briones, P., Leal, F., Pérez-Cerdá, C., Ribes, A., Ugarte, M., Pérez, B., and MMACHC Working Group (2009) Genetic and cellular studies of oxidative stress in methylmalonic aciduria (MMA) cobalamin deficiency type C (*cblC*) with homocystinuria (MMACHC). *Hum. Mutat.* **30,** 1558–1566
27. Yamanishi, M., Labunska, T., and Banerjee, R. (2005) Mirror "base-off" conformation of coenzyme B_{12} in human adenosyltransferase and its downstream target, methylmalonyl-CoA mutase. *J. Am. Chem. Soc.* **127,** 526–527
28. Mosharov, E., Cranford, M. R., and Banerjee, R. (2000) The quantitatively important relationship between homocysteine metabolism and glutathione synthesis by the transsulfuration pathway and its regulation by redox changes. *Biochemistry* **39,** 13005–13011
29. Takahashi, K. (1968) The reaction of phenylglyoxal with arginine residues in proteins. *J. Biol. Chem.* **243,** 6171–6179
30. Meister, A. (1995) Glutathione metabolism. *Methods Enzymol.* **251,** 3–7
31. Vitvitsky, V., Dayal, S., Stabler, S., Zhou, Y., Wang, H., Lentz, S. R., and Banerjee, R. (2004) Perturbations in homocysteine-linked redox homeostasis in a murine model for hyperhomocysteinemia. *Am. J. Physiol. Regul. Integr. Comp. Physiol.* **287,** R39–R46
32. Payne, K. A., Quezada, C. P., Fisher, K., Dunstan, M. S., Collins, F. A., Sjuts, H., Levy, C., Hay, S., Rigby, S. E., and Leys, D. (2015) Reductive dehalogenase structure suggests a mechanism for B_{12}-dependent dehalogenation. *Nature* **517,** 513–516
33. Bommer, M., Kunze, C., Fesseler, J., Schubert, T., Diekert, G., and Dobbek, H. (2014) Structural basis for organohalide respiration. *Science* **346,** 455–458
34. Armstrong, R. N. (1997) Structure, catalytic mechanism, and evolution of the glutathione transferases. *Chem. Res. Toxicol.* **10,** 2–18
35. Wang, R. W., Newton, D. J., Johnson, A. R., Pickett, C. B., and Lu, A. Y. (1993) Site-directed mutagenesis of glutathione *S*-transferase YaYa: mapping the glutathione-binding site. *J. Biol. Chem.* **268,** 23981–23985
36. Pal, A., Gu, Y., Herzog, C., Srivastava, S. K., Zimniak, P., Ji, X., and Singh, S. V. (2001) Role of arginine 216 in catalytic activity of murine Alpha class glutathione transferases mGSTAl-1 and mGSTA2–2 toward carcinogenic diol epoxides of polycyclic aromatic hydrocarbons. *Carcinogenesis* **22,** 1301–1305
37. Stenberg, G., Board, P. G., Carlberg, I., and Mannervik, B. (1991) Effects of directed mutagenesis on conserved arginine residues in a human Class Alpha glutathione transferase. *Biochem. J.* **274,** 549–555
38. Mc Guire, P. J., Parikh, A., and Diaz, G. A. (2009) Profiling of oxidative stress in patients with inborn errors of metabolism. *Mol. Genet. Metab.* **98,** 173–180
39. Ramasamy, S., Kundu, T. K., Antholine, W., Manoharan, P. T., and Rifkind, J. M. (2012) Internal spin trapping of thiyl radical during the complexation and reduction of cobalamin with glutathione and dithiothrietol. *J. Porphyr. Phthalocyanines* **16,** 25–38
40. Pastore, A., Martinelli, D., Piemonte, F., Tozzi, G., Boenzi, S., Di Giovamberardino, G., Petrillo, S., Bertini, E., and Dionisi-Vici, C. (2014) Glutathione metabolism in cobalamin deficiency type C (cblC). *J. Inherit. Metab. Dis.* **37,** 125–129
41. Bartholomew, D. W., Batshaw, M. L., Allen, R. H., Roe, C. R., Rosenblatt, D., Valle, D. L., and Francomano, C. A. (1988) Therapeutic approaches to cobalamin-C methylmalonic acidemia and homocystinuria. *J. Pediatr.* **112,** 32–39
42. Andersson, H. C., and Shapira, E. (1998) Biochemical and clinical response

to hydroxocobalamin versus cyanocobalamin treatment in patients with methylmalonic acidemia and homocystinuria (*cblC*). *J. Pediatr.* **132,** 121–124
43. Wood, P. M. (1988) The potential diagram for oxygen at pH 7. *Biochem. J.* **253,** 287–289
44. Lexa, D., and Saveant, J.-M. (1983) The electrochemistry of vitamin B_{12}. *Acc. Chem. Res.* **16,** 235–243
45. Suarez-Moreira, E., Yun, J., Birch, C. S., Williams, J. H., McCaddon, A., and Brasch, N. E. (2009) Vitamin B_{12} and redox homeostasis: cob(II)alamin reacts with superoxide at rates approaching superoxide dismutase (SOD). *J. Am. Chem. Soc.* **131,** 15078–15079
46. Peel, J. L. (1962) Vitamin B_{12} derivatives and the CO2-pyruvate exchange reaction: a reappraisal. *J. Biol. Chem.* **237,** PC263–PC265
47. Aronovitch, J., and Grossowicz, N. (1962) Cobalamin catalyzed oxidation of sulfhydryl groups. *Biochem. Biophys. Res. Commun.* **8,** 416–420
48. Schrauzer, G. N., and Sibert, J. W. (1969) Electron transfer reactions catalyzed by vitamin B_{12} and related compounds: the reduction of dyes and of riboflavin by thiols. *Arch. Biochem. Biophys.* **130,** 257–266
49. Madej, E., and Wardman, P. (2007) The oxidizing power of the glutathione thiyl radical as measured by its electrode potential at physiological pH. *Arch. Biochem. Biophys.* **462,** 94–102
50. Balagopalakrishna, C., Abugo, O. O., Horsky, J., Manoharan, P. T., Nagababu, E., and Rifkind, J. M. (1998) Superoxide produced in the heme pocket of the β-chain of hemoglobin reacts with the β-93 cysteine to produce a thiyl radical. *Biochemistry* **37,** 13194–13202